https://doi.org/10.5194/essd-2025-360
Preprint. Discussion started: 7 July 2025

Open Access Earth System Science Data Discussions

Atmospheric and Ocean CO_2 Measurements in the South Indian Ocean Made by Two Uncrewed Surface Vehicles in 2022 and 2023

Don P. Chambers[1], Jennifer Bonin[1], Adrienne Sutton[2], Roman Battisti[2], Stacy Maenner[2], Veronica Tamsitt[1,3], and Nancy Williams[1]

[1] College of Marine Science, University of South Florida, St. Petersburg, FL, USA

[2] National Oceanographic and Atmospheric Administration, Pacific Marine Environmental Laboratory, Seattle, WA, USA

[3] Submarine Scientific LLC, San Francisco, CA, USA

Correspondence to: Don P. Chambers (donc@usf.edu)

Abstract. During the second half of 2022 and the first several months on 2023, a pair of Uncrewed Surface Vehicles (USVs) collected high-resolution (~5-km sampling) measurements of ocean and atmosphere pCO_2, air temperature and humidity, wind, ocean skin temperature, sea surface temperature, salinity, ocean color (Chlorophyll α), dissolved oxygen, and ocean current velocity between roughly 13.5°E and 82°E and between the Subtropical Front (STF) and the Subantarctic Front (SAF). The mission track spanned from the Agulhas Return Current south of South Africa to the northern boundary of the Antarctic Circumpolar Current downstream of the Kerguelen Plateau. The primary goal of the mission was to collect data within cyclonic and anticyclonic eddies to quantify CO_2 fluxes to better understand physical processes (upwelling and downwelling) that that can contribute to carbon cycling in addition to the biological pump. In this paper, we present an overview of the mission, details on the data collected, and a preliminary look at calculated surface pCO_2, separated into cyclonic/anti-cyclonic/no-eddy conditions.

1 Introduction

The Southern Ocean south of 35°S plays a major role in the ocean carbon cycle and in Earth's climate system by accounting for ~40% of the total oceanic uptake of anthropogenic carbon dioxide (CO2) despite making up only 20% of the global ocean surface (Devries, 2014). This uptake of anthropogenic carbon occurs against a background of larger natural carbon fluxes which vary both seasonally and spatially across the Southern Ocean's diverse frontal regions. Interannual and decadal variability in Southern Ocean air-sea CO2 fluxes is significant (Landschützer et al., 2015) and drives overall variability in the global ocean carbon sink (Gruber et al., 2019).

Despite its importance in the global carbon cycle and the ongoing changes to winds, meltwater, temperature, and carbon content occurring there (e.g., Bronselaer et al., 2020; Toggweiler, 2009), the Southern Ocean is relatively under-sampled due

https://doi.org/10.5194/essd-2025-360
Preprint. Discussion started: 7 July 2025

to its remote and dangerous nature, leading to large uncertainties in ocean carbon uptake estimates. Predictions about how the ocean carbon sink will evolve under continued anthropogenic change are foiled by our inability to fully understand it in its present state.

In the last few decades, sparse historical shipboard measurements of the ocean's partial pressure of CO_2 (pCO_2) have been synthesized into data products such as the Surface Ocean CO_2 Atlas (SOCAT; Bakker et al., 2016). These products are then used along with sophisticated mapping techniques to quantify air-sea CO_2 fluxes and the strength of the ocean carbon sink over space and time. One such method is the self-organizing map feed-forward network (SOMFFN) of Landschützer et al. (2016). The SOMFFN incorporates sea surface temperature (SST), sea surface salinity, mixed layer depth, satellite chlorophyll, atmospheric CO_2, and the gridded SOCAT pCO_2 product to map monthly fields of surface ocean pCO_2 and air-sea fluxes over time and is updated approximately annually.

However, the largest concentration of observations occurred in the Northern Hemisphere, with many fewer observations taken in the Southern Ocean (e.g., Fig. 3 from Bakker et al., 2016). Additionally, measurements are biased toward the summer months in the Southern Ocean due to better ocean conditions for ship-based measurements.

Autonomous platforms provide opportunities for year-round observations of important parameters of the ocean chemistry, even in the rough conditions of the Southern Ocean. The Southern Ocean Carbon and Climate Observations and Modeling (SOCCOM) Project has deployed several hundred Biogeochemical (BGC)-Argo floats throughout the Southern Ocean since 2014 (Sarmiento et al., 2023), returning thousands of profiles of temperature, salinity, O_2, NO^3, and pH to depths of 2000 m approximately every 10 days. While pCO_2 can be derived from the BGC-Argo pH measurements and estimated total alkalinity, the measurements are expected to have a higher uncertainty than direct pCO^2 measurements, ~3% compared to 0.5%, along with a potential bias (Bushinsky et al., 2019; Williams et al., 2017).

Between January and August of 2019, an Uncrewed Surface Vehicle (USV) from Saildrone Inc. completed the first autonomous Antarctic circumnavigation (Sutton et al., 2021; 2023). It carried the NOAA PMEL-designed ASVCO2® package (Sabine et al., 2020**)** along with a suite of meteorological and oceanographic sensors (e.g., air and surface seawater temperature, salinity, chlorophyll fluorescence, and ocean currents), allowing highly accurate (±2 μatm) measurements of surface ocean and atmospheric pCO_2. Although the mission was primarily an engineering test to study the USV's endurance in the Southern Ocean's harsh conditions, data collected along the track suggested significant outward fluxes of CO_2 during austral winter and in regions along and south of the Polar Front where there is intense eddy activity (Fig. 2 of Sutton et al., 2021). Previous studies have theorized that mesoscale eddies could enhance or suppress the flux of CO_2 between the atmosphere and ocean due to the intense upwelling or downwelling caused by their circulation (McGillicuddy, 2016).

https://doi.org/10.5194/essd-2025-360
Preprint. Discussion started: 7 July 2025

This led us to propose another Saildrone USV mission, which was funded by the National Science Foundation in late 2020. We placed an instrument package identical to that used in the 2019 Antarctic Circumnavigation experiment (Sutton et al., 2023) on a Saildrone USV (designated SD1038), which was the primary platform for our mission. We additionally leveraged collaboration with the EU-funded Southern Ocean Carbon and Heat Impact for Climate (SO-CHIC) project (https://www.sochic-h2020.eu) which was planning to operate two Saildrone USVs in the Southern Ocean around the same time. They allowed us to place a matching CO_2-observing package on one of their two USV's (SD1039). Although we did not give our mission an acronym in the design or implementation phase, we have begun calling it the Southern Ocean Saildrone (SOS) mission, for reasons which will become clear shortly.

The plan was for all three SOS/SO-CHIC USVs to be launched from South Africa in the March to April 2021 timeframe. Two would sail to the SO-CHIC observation area (~10°E, 45°S), while SD1038 would sail to the SOS mission's initial observing area to the east and further south (Site A in Fig. 1), an eddy-rich area where the Subantarctic Fronts (SAF) and Polar Fronts (PF) often merge. The plan was for SD1038 to take observations of pCO^2, pH, and other parameters within a number of cyclonic and anticyclonic eddies beginning in May to June. Eddies would be identified in near-real-time maps of sea surface height anomalies observed by satellite altimeters (e.g., Chelton et al., 2007; Mason et al., 2014). After observing as many eddies as possible in the two-month window, SD1038 would transit along the Polar Front until it reached the eddy-rich region downstream of the Kerguelen Plateau (Site B in Fig. 1). SD1039, after making observations in the SO-CHIC region, was expected to follow SD1038 with a lag of 3-4 weeks, trying to sample the same eddies SD1038 had previously.

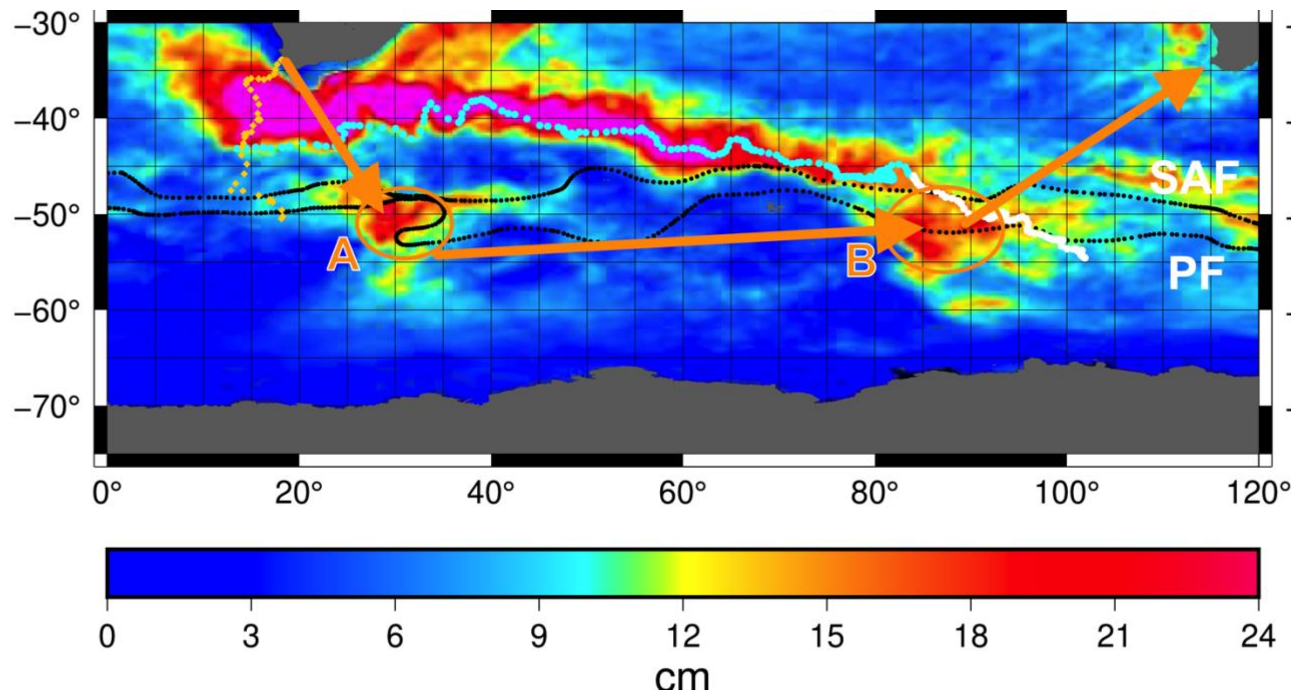

https://doi.org/10.5194/essd-2025-360
Preprint. Discussion started: 7 July 2025

Figure 1: Trajectories of SD1038 (orange diamonds) and SD1039 (cyan and white circles) on top of standard deviation of sea surface height variability (color contours), with the approximate positions of the Subantarctic Front (SAF) and Polar Front (PF) from Orsi et al. (1995) shown with black dots. The original planned trajectory and observation sites are shown in orange arrows and circles.

Early on, it became clear that the SOS mission plan would have to be altered. Due to closures of South Africa due to the COVID-19 pandemic, both the SOS and SO-CHIC missions were delayed by more than a year. SD1038 finally reached a site west of the initial observation area on July 19, 2022, many months in the season later than expected. However, it quickly became apparent that the wave-generator and solar cells were not recharging the batteries fast enough to keep up with the requirements from the instrumentation and navigation, so the USV was rapidly losing power. On July 23, a lower sampling rate was implemented to reduce power drain with a hope that the batteries could recharge. But by July 26, it was clear the hydrogenerator couldn't operate in the high sea state, and that the rudder or wing had been damaged (possibly by a rogue wave), limiting the ability to tack to the port side. Consequently, the USV was drifting south. All instruments were turned off to conserve power in an attempt to recover the drone, allowing only a short period of time for observations (Fig. 1).

Subsequently, both the SOS and SO-CHIC missions were reassessed. The two USVs for the SO-CHIC mission had departed South Africa significantly later than SD1038 and had just crossed the Agulhas Current when SD1038 was powered down to try to limp it back to port in Johannesburg. After numerous discussions between the SOS Mission team, the SO-CHIC principal investigator, and the Saildrone navigation team, it was decided that SD1039 would begin moving toward the eddy-rich area downstream of the Kerguelen Plateau, but at a latitude no further south than 45°S for several months until increasing summertime solar radiation became sufficient to keep the batteries charged via the solar panels. The "new" SOS mission began on September 1 when SD1039 turned on its instruments at approximately 42°S, 12°E (Fig. 1). In the meantime, all contact had been lost with SD1038. Its last known position was 51°S, 24°E.

The "new" SOS mission plan was to observe eddies of opportunity along the Subtropical Front (STF) while moving eastward as quickly as possible toward the second main observation area downstream of Kerguelen between the Subantarctic Front (SAF) and Polar Front (PF), where it was hoped the USV could sample individual eddies over a slightly longer period. SD1039 reached a region just north of the proposed sampling area (B in Fig. 1) in early January 2023, but by the end of the month (January 26) it was clear that it was becoming more difficult to navigate the USV and that complex maneuvering (i.e.: targeting of specific eddies and intentionally sampling in patterns inside them) in the high sea-state was not possible. Efforts were made to steer the drone to Australia for recovery. Unfortunately, it became clear that the drone would not be recovered (like SD1038), and so the majority of the instruments were turned off on February 27, 2023.

https://doi.org/10.5194/essd-2025-360
Preprint. Discussion started: 7 July 2025

Fortunately, most observations had been uploaded in near-real-time throughout the mission, primarily to be used for measurement assessment and to aid in directing the USV, so we are able to report and archive the primary science measurements of both SD1038 and SD1039. Interestingly, the ASVCO_2 system (Sabine et al., 2020) continued to operate after most of the other instruments were turned off, until April 27, 2023, presumably because Saildrone could not power it down or its independent battery system maintained sufficient charge to take observations and transmit them. Therefore, hourly data for some variables (including positions from an onboard GPS receiver) continued to be shared with the data server at the NOAA Pacific Marine Environmental Laboratory (PMEL).

While the amount of data, locations, and timing of CO_2 measurements made from the two USVs as part of the SOS mission were not as anticipated, they still represent important direct observations of the carbon system in a poorly sampled region of the ocean. In this paper, we will describe the principal results of the mission, including how we deduced eddy matchups. Section 2 will provide an overview of the instruments onboard and the data collected, the methodology for determining eddy matchups, and describe where the data are permanently archived and how they can be accessed. Section 3 will discuss results from the primary CO_2 measurement system, showing derived atmospheric and ocean pCO_2 values along the tracks, discuss when the track was in an eddy, and provide some brief analysis of the results within eddies compared to when the USVs were not in an eddy. However, a thorough scientific analysis is beyond the scope of this paper and is left for further studies. This document is primarily intended to provide an overview of the data and mission.

2 Instrumentation and Data Collected

The Saildrone Uncrewed Surface Vehicle (USV) is an autonomous ocean data collection platform designed for long range, long duration missions of up to 12 months. Saildrone USVs run solely on renewable energy, using wind power for propulsion and solar energy and wave generators to run a suite of science-grade sensors. Each vehicle consists of a 7 m narrow hull, a maneuverable wing for sailing, and a keel with a 2.5 m draft. The USV weighs approximately 750 kg and can be launched and recovered from a dock. The USVs used in this mission are modified versions for the one used in the 2019 circumnavigation of Antarctica (Sutton et al., 2021). Anyone interested in specifics on Saildrone USVs should refer to that paper and all relevant references within it. The only major change to the USVs used for the SOS mission was a shorter and hardened wing designed to accommodate higher waves and winds in our mission area (Ricciardulli et al., 2022; Chiodi et al., 2023).

There is a suite of science grade sensors on each Saildrone platform to measure key atmospheric and oceanographic environmental variables (Table 1). These include solar irradiance, longwave radiation, atmospheric pressure, air temperature and humidity, wind speed and direction, ocean skin temperature, sea surface temperature (SST), salinity, ocean color

https://doi.org/10.5194/essd-2025-360
Preprint. Discussion started: 7 July 2025

(Chlorophyll α), and dissolved oxygen, among others (Zhang et al., 2019). The basic atmospheric and oceanographic data were sampled at hourly or sub-hourly intervals for SD1038's entire record and for 1 September 2022 through 27 February 2023 for SD1039 (the cyan portion of the trajectory shown in Fig. 1), after which point the sampling systems were turned off to conserve power.

Table 1: **Primary measurements on SD1038 and SD1039, including instrument type and special notes on placement or availability.**

Measurements (incl. Variable Names in Datafiles)	**Instrument**	**Notes**
wind parameters (WIND_U, WIND_V, WIND_W, WIND_SPEED, WIND_GUST, WIND_FROM_DIR)	Gill model 1590-PK-020 anemometer	Wind values measured at ~3.4 meters above local sea level
Satellite wind speed (CCMP_WIND_EAST, CCMP_WIND_NORTH, CCMP_WIND_SPEED)	Cross-Calibrated Multi-Platform (CCMP) Wind Vector analysis	Interpolated from 0.25°, 6-hour grids.
Atmospheric temperature/humidity (ATM_TEMP, ATM_REL_HUMID)	Rotronic model HC2-S3 standard meteorological probe	Install height: 2.3 m
Photosynthetically Active Radiation (PAR)	LI-COR model LI-192SA underwater quantum sensor	
Incoming Shortwave Radiation (IRRAD_SW_DIFFUSE, IRRAD_SW_TOTAL)	Delta-T model SPN1-shaded shaded pyranometer	Only on SD1039
Outgoing longwave radiation (IRRAD_LW)	Eppley model PIR infrared radiometer	Only on SD1039
Atmospheric Pressure (ATM_PRESS)	Valsala model PTB210 barometer	Install height: 0.2 m
Seawater properties (SW_COND, SW_TEMP, SW_SAL, O2_SAT, O2_CONC)	Sea-Bird Scientific model SBE37-SMP-ODO microCAT conductivity, temperature, and optical pressure recorder with dissolved oxygen sensor	Install height: -0.5 m
Skin temperature (SW_TEMP_SURFACE_SKIN)	Heitronics model CT15.10 infrared radiation thermometer	Install height: 2.3 m
Chlorophyll (CHLOR)	WET Labs model FLS fluorometer	Install height: -0.5 m
Longitude/Latitude, wave characteristics	VectorNav model VN-300 GNSS-aided inertial navigation system	

https://doi.org/10.5194/essd-2025-360
Preprint. Discussion started: 7 July 2025

(WAVE_DOM_PERIOD, WAVE_SIG_HEIGHT)		
Water velocity (VEL_EAST, VEL_NORTH, VEL_UP)	Teledyne model Workhorse WHM300-I-UG1 acoustic doppler current profiler (ADCP)	Install height: -1.9 m SD1038: never turned on SD1039: intermittently on during mission
Atmospheric/Ocean Chemistry (ATM_fCO2, ATM_H2O, ATM_pCO2, ATM_PRESS_LICOR, ATM_TEMP_LICOR, ATM_xCO2_DRY, ATM_xCO2_WET, O2_RATIO, DIFF_fCO2, DIFF_pCO2, SW_fCO2, SW_H2O, SW_pCO2, SW_xCO2_DRY, SW_xCO2_WET)	ASVCO_2 with Licor model LI-820 gas analyzer	Install heights: 1.3 m (air) and -0.5 m (ocean) Included separate GNSS system for recording positions

The vehicles used for the SOS mission were also equipped with acoustic doppler current profilers (ADCP). However, the ADCP was never turned on for SD1038 due to power consumption problems and was on intermittently for SD1039 due to several issues. No ADCP data was collected before 26 September 2022, or from 18 October 2022 1530 UTC to 26 October 2022 0 UTC. Additionally, between 26 September 2022 1700 UTC and 12 October 2022 2100 UTC, the ADCP data is flagged as "bad" within the datafile and should be used with caution, because the ADCP was accidentally switched to bottom tracking mode in deep water during this period.

Although both USVs had an anemometer to directly measure wind conditions, the system failed early in the SD1039 leg (on 2 September 2022). Because of this, we have also included windspeed computed from a statistical combination of satellite-based vector winds and atmospheric re-analyses, the Cross-Calibrated Multi-Platform (CCMP) Wind Vector analysis product (https://www.remss.com/measurements/ccmp/; Mears et al., 2022a,b). These data, collocated at USV times and locations, are included even when the anemometer winds are available so users can have a consistent wind data set and can compare in situ and satellite-based wind speed.

The primary instrument package for this mission was the ASVCO_2 system (Sabine et al., 2020), identical to the system deployed on the 2019 Saildrone mission (Sutton et al., 2021). The ASVCO_2 system is capable of measuring surface ocean and atmosphere pCO_2 to within ± 2 µatm (± 0.5%) by performing a calibration before every measurement with a zero and an on-board CO_2 gas standard and have been used on over a dozen missions. For anyone interested in details on how the system works and the exact processing steps to convert between measured variables and derived variables, we refer you to Sutton et al. (2014) and Sabine et al. (2020).

To be consistent with the $ASVCO_2$ sensor data distributed with the 2019 Saildrone mission, the SD1038 and SD1039 $ASVCO_2$ data are archived at the NOAA National Centers for Environmental Information (NCEI) (Chambers et al., 2025a,b) in the same format and with the same processing as done for previous USV-based surface ocean pCO_2 data. The raw wet xCO_2 data, temperature, salinity, and pressures are included so other data users can recalculate dry xCO_2, fCO_2, and pCO_2. While the $ASVCO_2$ sensor package also included a DuraFET pH sensor, these data are not included in the files as they are uncalibrated. They were only used in quality checking and flagging of CO_2 measurements.

The two $ASVCO_2$ datasets do not contain all the ancillary data measured by other Saildrone USV instruments, nor do they contain any sub-hourly observations, since the system was not linked to the transfer system used to download the other observations via satellite link. Because of this, we have created a third dataset that includes all the $ASVCO_2$ variables in the two NCEI files as well as all other available observations from each of the two USVs (Chambers et al., 2025c). The only exception is the segment of SD1039 shown in white in Fig. 1. These data come from only the $ASVCO_2$ system; other sampling systems had been turned off to conserve power at this point. The measurements relevant to the chemistry data for that short leg are available in the NCEI archive (Chambers et al., 2025a), including positions recorded by a GPS internal to the $ASVCO_2$. Because there was not a full suite of measurements, including such key parameters as ocean temperature and salinity, as in the primary mission (cyan track in Figure 1), this later CO_2-related data are not included in the full mission datafile for SD1039. The details of the datafiles (including archive location) are given in Table 2.

Table 2: Archived Data Files (including locations and important differences)

Datafile	Location	Notes
SD1038 Chemistry Data	https://doi.org/10.25921/r2mt-t398	Measured and derived parameters from the $ASVCO_2$ system
SD1039 Chemistry Data	https://doi.org/10.25921/6b0k-r665	Measured and derived parameters from the $ASVCO_2$ system
SD1038/1039 Full Mission Data	https://doi.org/10.17632/9ymsjsyhhp.1	Chemistry and other physical measurements not in the Chemistry Data files. Hourly data for all, sub-hourly for some.

The observables listed in Table 1 were sampled at various rates. For example, the $ASVCO_2$ returned a measurement based on a several minute average at 16 minutes after each hour. Other observations made using the primary Saildrone USV instrumentation packages were transmitted on more frequent intervals, some as frequently as every minute, some 10-15 times each hour. Each reported sample is the average of ~11 observations taken in a planned burst, over an 11-second span centered at the top of the minute reported. To account for the different sampling rates, we have created two types of data files

https://doi.org/10.5194/essd-2025-360
Preprint. Discussion started: 7 July 2025

for users in the full mission data set (Table 2): one with one-minute sampling, the other with one-hour averages. The one-minute files have many missing records due to the non-constant sampling (e.g., for the chemical variables, only one per hour). Where available, the standard deviation of the 11-second burst measurement is also included. Because the majority of data types do not vary rapidly within an hour, we additionally made a smaller hourly-averaged files, based on averages of the sub-hour sampled files. For the air and seawater CO_2 variables where there was only one observation within that hour only that single value is given, so it is not a true hourly average.

Because the goal of the SOS mission was to measure pCO_2 within different eddies, we have also provided an estimate of whether the USV was in an eddy or not, along with the type of eddy (cyclonic, anticyclonic) in the main mission datafile. This was not done for SD1038 as the drone lost power before we could intentionally maneuver it into any eddies, but has been done for SD1039. Eddy direction is determined using a database of eddy positions and sizes that are provided in the regularly updated near-real-time Mesoscale Eddy Trajectory Atlas, distributed by the E.U. Copernicus Marine Service/CNES/CLS, based on satellite altimetry estimates of absolute dynamic topography using the detection methods of Mason et al. (2014). The eddy database contains all the statistics of the eddy necessary for this study: the time, location of the center, the amplitude of sea level anomaly in the center, radius of the eddy from the center to where the velocity is the maximum (r_{max}), and the maximum velocity.

We describe SD1039 as being "inside" an eddy if the distance between SD1039 and the reported center of the eddy is less than the reported radius of that eddy on the same day that the USV passed through it. Additionally, we require the USV to remain within the radius of the (moving) eddy for at least 24 hours. The latter constraint was required to prevent four very short (2-17 hour) eddy "intersections" which occurred as the distance from the eddy center to SD1039 approached the eddy radius. Investigations using SD1039's ADCP data did not support the presence of an eddy in these cases, so they were rejected. Additionally, in the case of the first cyclonic eddy, it appeared that SD1039 moved into the eddy, out of it, and then back in. Upon investigation, this odd behavior was caused by an atypically large shift of the eddy's position between one day's database record and the next, which is unlikely to be realistic. In our product, we thus define all times between the initial entrance and final exit of that eddy to be "in an eddy", even when the database says it is slightly outside the radius of the eddy. Altogether, SD1039 traveled through 12 eddies as defined by these criteria, of which 9 were anticyclonic and 4 were cyclonic (Fig. 2). However, only 8 of the anticyclonic eddies have CO_2 measurements – the first eddy at the start of the transit has no valid $ASVCO_2$ measurements.

https://doi.org/10.5194/essd-2025-360
Preprint. Discussion started: 7 July 2025

Open Access Earth System Science Data Discussions

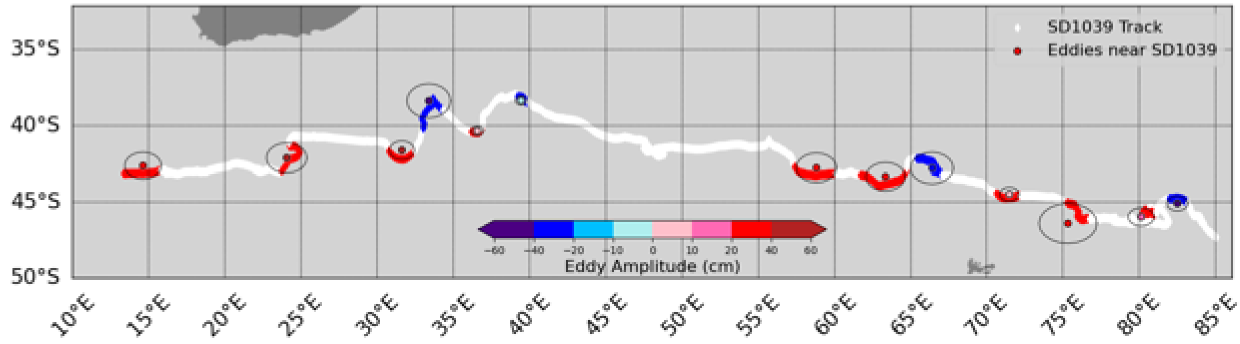

Figure 2: **Trajectory of SD1039 with nearby eddies as found via matchups with an altimeter-based eddy atlas. Track colors represent periods when SD1039 was in a region of no eddies (white), an anticyclonic eddy (red), or a cyclonic eddy (blue). Center locations of expected eddies from the database, averaged over the period SD1039 is nearby, are shown as dots, with dot color representing average database amplitude and black circles denoting the average radius of each eddy.**

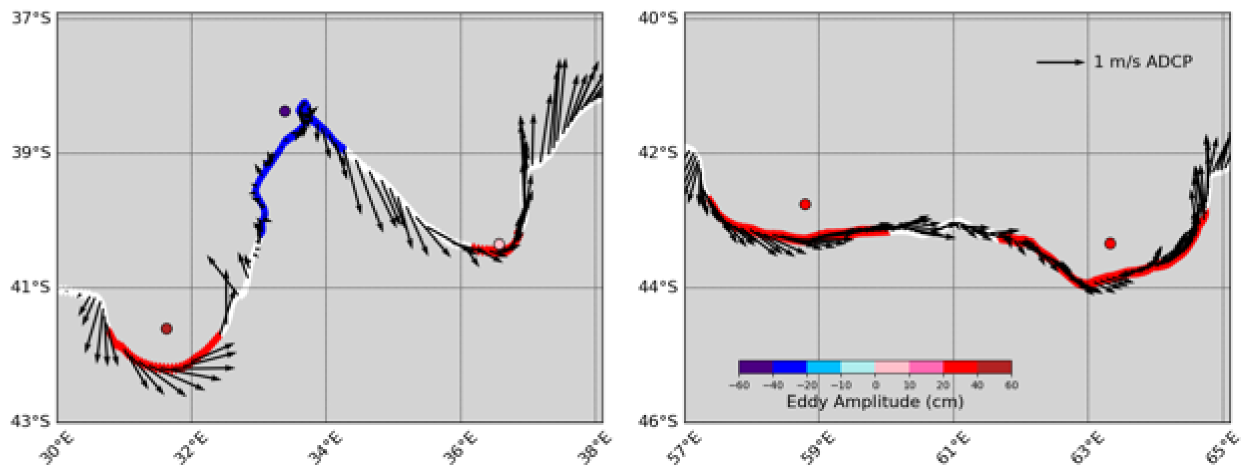

Figure 3: Surface ADCP velocities (vectors) from SD1039, along with the SD1039 track colored in the same manner as in Figure 2. Red colors indicate a nearby expected anti-cyclonic eddy, while blue colors indicate a nearby cyclonic eddy. Colored circles show the expected mean center of eddy rotation and its amplitude, averaged over the time SD1039 was inside it, based on the eddy database.

The eddy database is capable of detecting only large eddies (diameters > 100-200 km), due to the use of gridded, optimally interpolated altimetry data in its construction. We anticipate that SD1039 likely passed through additional smaller eddies on its path. We attempted to use the ADCP data to detect rotations associated with such eddies, but found that impossible using a single track of ADCP data. However, with additional work (e.g., removing some climatological currents to obtain anomalous velocity and removing non-geostrophic Ekman currents using wind fields), more eddy-related information might be teased out of this ADCP data/ Therefore, we include the ADCP velocity information in the data files for users to experiment with.

3 Analysis of Chemistry Data

Here we only analyze the most novel observations from the SOS mission, the pCO_2 measurements (air and sea), and present a preliminary analysis of observed variations that may correlate with the eddy-type (Fig. 4). The most obvious signal in measured pCO_2 by SD1038 during its June-July transit from South Africa is an increase in pCO_2 values from ~350 µatm at 35° S to ~405 µatm at 50° S as the vehicle moved southwards (Fig. 4a and 4b). These values are within an expected range, as Shadwick et al. (2023) documented seasonal variations at a similar latitude in a mooring south of Tasmania with a peak (380-400 µatm) around July/August.

Comparing the pCO_2 to a mean monthly climatology (Fig. 5) we confirm the shift in values of pCO_2 in SD1038 around 45°S is consistent with the mean state in that region for the time of year. We do note a bias between the measurements of both SD1038 and SD1039 and the climatology (Fig. 5) of approximately 20-25 µatm (SD1038/1039 higher). While it is beyond the scope of this paper to understand the bias, it may be due to limited data in the region used for the climatology, a real interannual variation, or different models for constructing pCO_2. The latter should be resolvable by users of the SD1038/SD1039 data, as all the measured observations are available in the archived data to produce pCO_2 based on any model the authors choose.

https://doi.org/10.5194/essd-2025-360
Preprint. Discussion started: 7 July 2025

Open Access Earth System Science Data Discussions

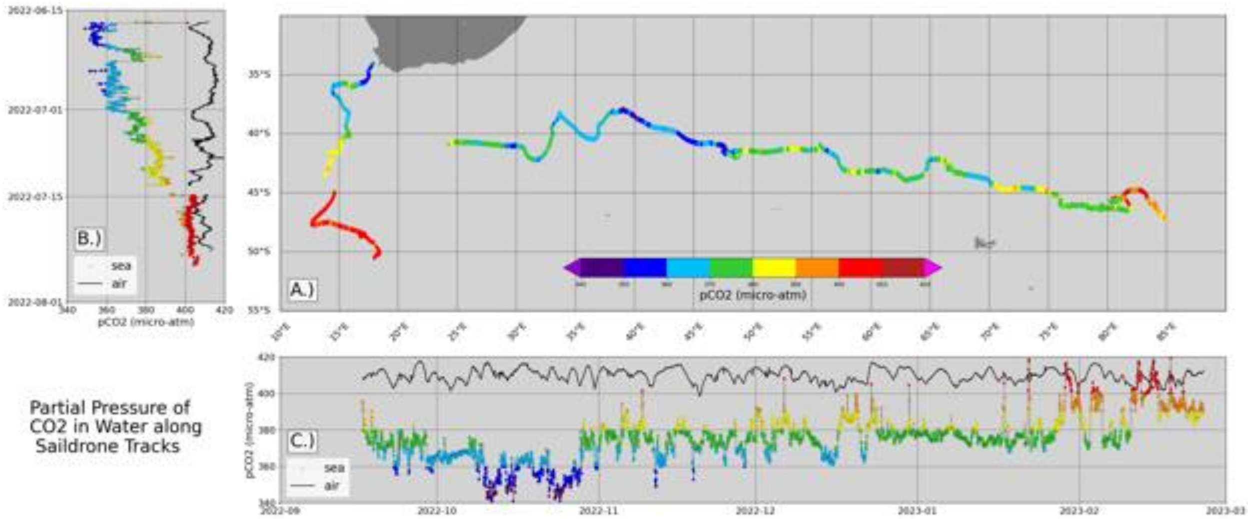

Figure 4: **a) Observed ocean pCO_2 along the transects of SD1038 and SD1039. Also shown versus time for SD1038 (b) and SD1039 (c), along with atmospheric pCO_2 (black dots)**.

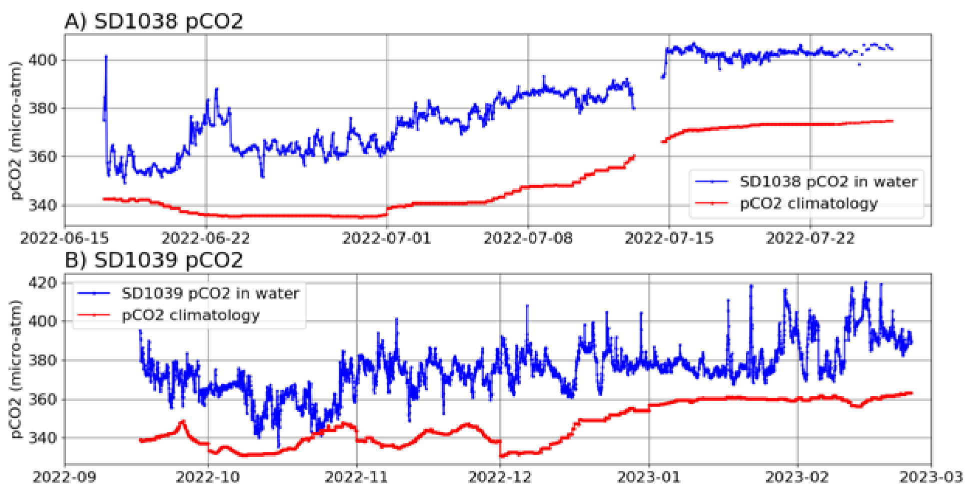

Figure 5: **Observed ocean pCO_2 along the transects of SD1038 (a) and SD1039 (b). Also shown are values from a mean seasonal climatology (red, data from Landschützer et al., 2020a,b). The climatology is based on all available data from 1 Jan. 1988 to 1 Jan. 2020.**

The ocean pCO_2 along the SD1039 track (Fig. 4a,c) primarily varies between 360 – 385 µatm, except for short excursions where the water pCO_2 abruptly drops or rises by up to 20 µatm for a period lasting less than a day (in most cases, only a few hours). Some spikes are larger than +40 µatm near the end of the record, indicating a short-term higher concentration of

https://doi.org/10.5194/essd-2025-360
Preprint. Discussion started: 7 July 2025

Open Access Earth System Science Data Discussions

pCO_2 in the surface waters than in the atmosphere. This suggests the potential for outgassing of CO_2 from the ocean to the atmosphere during these periods, but more work would be required to fully quantify this.

The extended drop in ocean pCO_2 in October 2022, when values reached as low as 340 µatm occurred around latitude 40° S and between 37° E and 47° E. At the same time, there was a steady rise in Chlorophyll α (Chl), rising to the maximum values observed during the transect (> 20 mg/l, averaged over 2 days) (Fig. 6). The time of transit was austral spring, when phytoplankton blooms tend to be frequent (e.g., Bathmann et al., 1997). While the minimum pCO_2 does not occur at the same time as maximum Chl, we also have no direct measure of the age or evolution of the possible phytoplankton bloom in the area. Because SD1039 transited near the middle of the austral spring, it is possible that the drop in ocean pCO_2 is related to a previous spike in Chlorophyll α (phytoplankton) concentration. We note this as a potential area of interest for future studies, as it might be possible to derive a time-series of Chlorophyll α for this area using satellite ocean color observations. That is, however beyond the scope of this study.

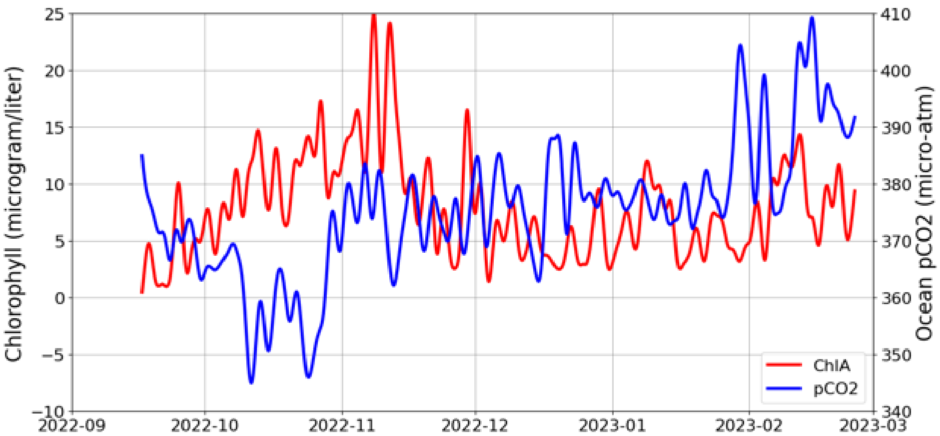

Figure 6: Low-pass filtered ocean pCO_2 (blue, right scale) and Chlorophyll α (red, left scale) along SD1039 transect. The low-pass filter was a Gaussian smoother with a roll-off of 24 hours, which effectively suppresses variations with periods shorter than 2-days.

We considered whether there was any relationship between abrupt changes in ocean pCO_2 and SD1039's location within an eddy (Fig. 7) but found no correlation between the magnitude of change or direction with being in an eddy or the type of eddy, even near the end of the transect when the variations are larger. For example, while there is a significant increase in ocean pCO_2 during the transect of anticyclonic eddy 6 (AC6), during other transects (AC2, 3, 7, 8) there are either no major changes, or even decreases in pCO_2.

The low number of cyclonic eddy transects does not allow any robust statistical comparisons, but qualitatively we find no

https://doi.org/10.5194/essd-2025-360
Preprint. Discussion started: 7 July 2025

consistent pattern. While there is a small increase in pCO_2 in cyclonic eddy 2 (C2) up from the minimum values likely connected with a phytoplankton bloom, this does not occur in C1. In the long transit of C3, there are rises and falls of pCO_2. The largest multi-day increase in pCO_2 occurs outside an eddy in early 2003 (just before entering AC8).

While these results are not conclusive that upwelling/downwelling in eddies has no effect on ocean pCO_2, it is apparent it is at most a second order effect compared to other processes along the USV transit during the austral spring and summer. This is not surprising, as biological interactions are strong during this period.

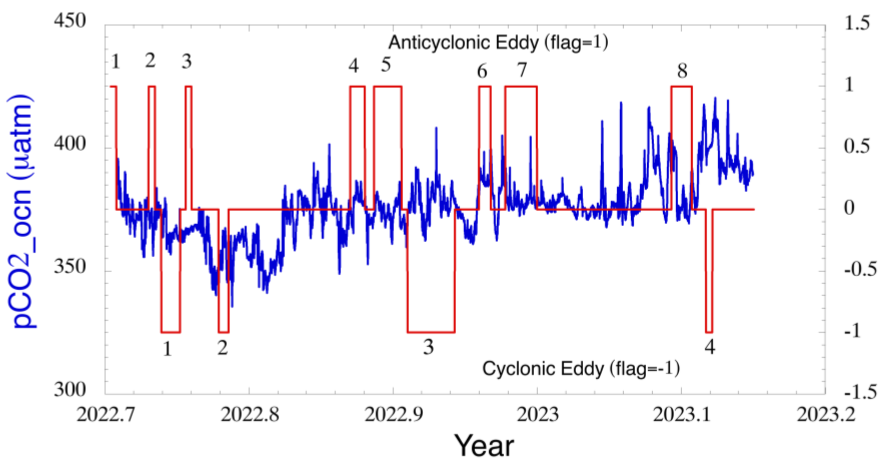

Figure 7: Ocean pCO_2 (blue) along SD1039 transect and eddy flag values (red). Flags with value =1 indicate an anticyclonic eddy, while value=-1 indicates the drone was in a cyclonic eddy.

4 Data Availability

All data are available from public archives. The observations (and derived chemistry variables) from the two $ASVCO_2$ system are stored in two files, separated by the designation of the USV: SD1039 (https://doi.org/10.25921/6b0k-r665; Chambers et al., 2025a) and SD1038 (https://doi.org/10.25921/r2mt-t398; Chambers et al., 2025b). These data are in CSV format (identical to previously released $ASVCO_2$ data from a previous (2019) USV mission (Sutton et al., 2020). A third set of files (in netCDF format) includes both datasets as well as additional ocean and atmospheric observations (e.g., those not listed as Atmospheric/Ocean Chemistry in Table 1): https://doi.org/10.17632/9ymsjsyhhp.1; Chambers et al., 2025c). This combined, full mission dataset also includes hourly averages and sub-hourly data (when available) and flags for whether the USV was in an eddy and the type of eddy.

https://doi.org/10.5194/essd-2025-360
Preprint. Discussion started: 7 July 2025

5 Conclusions

While the original goals and design of the SOS mission had to change dramatically due to outside circumstances, the team modified the mission goals to obtain as many useable atmospheric and oceanic observations as possible, in regions of the south Indian Ocean that are rarely sampled. Instead of simply navigating SD1039 back to South Africa after the problems encountered with SD1038, we attempted to navigate SD1039 to an eddy-rich area downstream of the Kerguelen Plateau between the Polar and Subantarctic Fronts, albeit along a more northerly route than planned and during the austral spring and summer, not winter.

SD1039 did transit through a handful of cyclonic and anti-cyclonic eddies, collecting novel CO_2 measurements. Although we were not successful in sampling eddies in a systematic manner (or with any time delay using two USVs), these measurements will contribute to a growing database of such data within eddies in the Southern Ocean (e.g., Keppler et al., 2025). The SOS team hopes that the small (but high-resolution) observations collected by SD1038 and SD1039 during the mission will aid future investigations in better understanding the physical processes that help control carbon cycling in the Southern Ocean.

Author Contributions

D. Chambers managed day-to-day science operations and collection during the missions and supervised analysis and archiving post-mission. He also wrote much of this data description document. J. Bonin provided analysis of eddies during the mission and handled the post-mission processing of the non-ASVCO_2 data. She also helped in producing figures for the manuscript and in the eddy-matchup analysis post-mission, and also co-wrote Sect. 2. A. Sutton, S. Maenner, and R. Battisti performed post-mission processing and quality control of the ASVCO_2 data and added commentary on the analysis of the results. V. Tamsitt aided in underway science operations, in the eddy match-up algorithms, and in writing the Introduction material. N. Williams conceived the mission, wrote the original proposal, and co-wrote the Introduction material with D. Chambers and A. Sutton.

Acknowledgements

We would like to thank the engineers at Saildrone, Inc. for managing the Saildrone USVs under challenging conditions and downloading as much data as possible when it was clear SD1039 would not be recovered (in particular, Julia Paxton and Matt Womble). The altimetric Mesoscale Eddy Trajectories Atlas (META3.2exp NRT) is produced by SSALTO/DUACS

https://doi.org/10.5194/essd-2025-360
Preprint. Discussion started: 7 July 2025

and distributed by AVISO+(https://www.aviso.altimetry.fr/en/data/products/value-added-products/global-mesoscale-eddy-trajectory-product/meta3-2-exp-nrt.html) with support from CNES, in collaboration with IMEDEA. This research was carried out under grant number 2048840 from the National Science Foundation. This is PMEL contribution 5766.

References

Bakker, D. C. E., Pfeil, B., Landa, C. S., Metzl, N., O'Brien, K. M., Olsen, A., et al.: A multi-decade record of high-quality fCO2 data in version 3 of the Surface Ocean CO2 Atlas (SOCAT). Earth System Science Data, 8, 383-413. https://doi.org/10.5194/ essd-8-383-2016, 2016.

Bathmann, U. V., Scharek, R., Klaas, C., Dubischar, C.D., Smetacek, V.: Spring development of phytoplankton biomass and composition in major water masses of the Atlantic sector of the Southern Ocean. Deep Sea Research Part II, 44, pp 51-67, https://doi.org/10.1016/S0967-0645(96)00063-X, 1997.

Bronselaer, B., Russell, J. L., Winton, M., Williams, N. L., Key, R. M., Dunne, J. P., et al.: Importance of wind and meltwater for observed chemical and physical changes in the Southern Ocean. Nature Geoscience, 13(1), 35–42. https://doi.org/10.1038/s41561-019- 0502-8, 2020.

Bushinsky, S. M., Landschützer, P., Rödenbeck, C., Gray, A. R., Baker, D., Mazloff, M. R., et al.: Reassessing Southern Ocean Air-Sea CO 2 Flux Estimates With the Addition of Biogeochemical Float Observations. Global Biogeochemical Cycles, 53(9). https://doi.org/10.1029/2019GB006176, 2019.

Carter, B. R., Williams, N. L., Gray, A. R., & Feely, R. A.: Locally interpolated alkalinity regression for global alkalinity estimation. Limnology and Oceanography: Methods, 14(4), 268–277. https://doi.org/10.1002/lom3.10087, 2016.

Carter, B. R., Feely, R. A., Williams, N. L., Dickson, A. G., Fong, M. B., & Takeshita, Y.: Updated methods for global locally interpolated estimation of alkalinity, pH, and nitrate. Limnology and Oceanography: Methods, 16(2), 119–131. https://doi.org/10.1002/lom3.10232, 2018.

Chai, F., Johnson, K.S., Claustre, H. et al.: Monitoring ocean biogeochemistry with autonomous platforms. *Nat Rev Earth Environ* **1**, 315–326. https://doi.org/10.1038/s43017-020-0053-y, 2020.

Chambers, Don P., Bonin, Jennifer, Tamsitt, Veronica, Williams, Nancy L., Sutton, Adrienne J., Maenner Jones, Stacy, Battisti, Roman, Osborne, John, Bott, Randy: Surface underway measurements of partial pressure of carbon dioxide (pCO2), sea surface temperature, sea surface salinity and other parameters from Autonomous Surface Vehicle (ASV) Saildrone 1039 (EXPOCODE 316420220901) in the Indian Ocean, Southern Ocean from 2022-09-01 to 2023-04-27 (NCEI Accession 0300658). [indicate subset used]. NOAA National Centers for Environmental Information. Dataset. https://doi.org/10.25921/6b0k-r665. Accessed [date], 2025a

Chambers, Don P.; Bonin, Jennifer; Tamsitt, Veronica; Williams, Nancy L.; Sutton, Adrienne J.; Maenner Jones, Stacy; Battisti, Roman; Osborne, John; Bott, Randy: Surface underway measurements of partial pressure of carbon dioxide (pCO2), sea surface temperature, sea surface salinity and other parameters from Autonomous Surface Vehicle (ASV) Saildrone 1038 (EXPOCODE 316420220616) in the Indian Ocean, Southern Ocean from 2022-06-16 to 2022-07-26 (NCEI Accession

0302848). [indicate subset used]. NOAA National Centers for Environmental Information. Dataset. https://doi.org/10.25921/r2mt-t398. Accessed [date], 2025b.

Chambers, Don; Bonin, Jennifer; Caggiano, Jessica; Williams, Nancy; Tamsitt, Veronica: Physical and chemical surface observations in the South Indian Ocean from two uncrewed sailing vehicles. Version 1.0. University of South Florida. https://doi: 10.17632/9ymsjsyhhp.1. Accessed [date], 2025c.

Chelton, D. B., Schlax, M. G., Samelson, R. M., & de Szoeke, R. A: Global observations of large oceanic eddies. Geophysical Research Letters, 34(15), 1–5. https://doi.org/10.1029/2007GL030812, 2007.

Chiodi, A. M., Hristova, H., Foltz, G. R., Zhang, J. A., Mordy, C. W., Edwards, C. R., et al.: Surface ocean warming near the core of hurricane Sam and its representation in forecast models. Frontiers in Marine Science, Volume 10 - 2023. https://doi.org/10.3389/fmars.2023.1297974, 2024.

Devries, T.: The oceanic anthropogenic CO2 sink: Storage, air-sea fluxes, and transports over the industrial era. Global Biogeochemical Cycles, 28(7), 631–647. https://doi.org/10.1002/2013GB004739, 2014.

Frenger, I., Münnich, M., Gruber, N., & Knutti, R.: Southern Ocean eddy phenomenology. Journal of Geophysical Research: Oceans, 120, 7413–7449. https://doi.org/10.1002/2015JC011047, 2015.

Friedlingstein, P., Jones, M. W., O'Sullivan, M., Andrew, R. M., Hauck, J., Peters, G. P., et al.: Global carbon budget 2019. Earth System Science Data, 11(4), 1783–1838. https://doi.org/10.5194/essd-11-1783-2019, 2019.

Gaube, P., Chelton, D. B., Strutton, P. G., & Behrenfeld, M. J.: Satellite observations of chlorophyll, phytoplankton biomass, and Ekman pumping in nonlinear mesoscale eddies. Journal of Geophysical Research: Oceans, 118(12), 6349–6370. https://doi.org/10.1002/2013JC009027, 2013.

Gaube, P., Chelton, D. B., Samelson, R. M., Schlax, M. G., & O'Neill, L. W.: Satellite Observations of Mesoscale Eddy-Induced Ekman Pumping. Journal of Physical Oceanography, 45(1), 104–132. https://doi.org/10.1175/JPO-D-14-0032.1, 2015.

Gray, A. R., Johnson, K. S., Bushinsky, S. M., Riser, S. C., Russell, J. L., Talley, L. D., et al.: Autonomous Biogeochemical Floats Detect Significant Carbon Dioxide Outgassing in the High-Latitude Southern Ocean. Geophysical Research Letters, 9049–9057. https://doi.org/10.1029/2018GL078013, 2018.

Gregor, L., Lebehot, A. D., Kok, S., & Scheel Monteiro, P. M.: A comparative assessment of the uncertainties of global surface ocean CO2 estimates using a machine-learning ensemble (CSIR-ML6 version 2019a) - Have we hit the wall? Geoscientific Model Development, 12(12), 5113–5136. https://doi.org/10.5194/gmd-12-5113-2019, 2019.

Gruber, N., Landschützer, P., & Lovenduski, N. S.: The Variable Southern Ocean Carbon Sink. Annual Review of Marine Science, 11(1), annurev-marine-121916-063407. https://doi.org/10.1146/annurev-marine-121916-063407, 2019.

Johnson, K. S., Jannasch, H. W., Coletti, L. J., Elrod, V. A., Martz, T. R., Takeshita, Y., et al.: Deep-Sea DuraFET: A Pressure Tolerant pH Sensor Designed for Global Sensor Networks. Analytical Chemistry, 88(6), 3249–3256. https://doi.org/10.1021/acs.analchem.5b04653, 2016.

Johnson, K. S., Plant, J. N., Coletti, L. J., Jannasch, H. W., Sakamoto, C. M., Riser, S. C., et al.: Biogeochemical sensor performance in the SOCCOM profiling float array. Journal of Geophysical Research: Oceans, 122(8), 6416–6436. https://doi.org/10.1002/2017JC012838, 2017.

Keppler, L., Eddebbar, Y. A., Gille, S. T., Guisewhite, N., Mazloff, M. R., Tamsitt, V., et al.: Effects of mesoscale eddies on southern ocean biogeochemistry. AGU Advances, 5, e2024AV001355. https://doi.org/10.1029/2024AV001355, 2024.

Landschützer, P., Gruber, N., & Bakker, D. C. E.: An observation-based global monthly gridded sea surface pCO2 product from 1998 through 2011 and its monthly climatology. Global Biogeochemical Cycles. Oak Ridge, Tennessee. https://doi.org/10.3334/CDIAC/OTG.SPCO2_1982_2011_ETH_SOM-FFN, 2015.

Landschützer, Peter, Gruber, N., & Bakker, D. C. E.: Decadal variations and trends of the global ocean carbon sink. Global Biogeochemical Cycles, 30(10), 1396–1417. https://doi.org/10.1002/2015GB005359, 2016.

Landschützer, P., Laruelle, G. G., Roobaert, A., and Regnier, P.: A uniform pCO2 climatology combining open and coastal oceans, Earth Syst. Sci. Data, 12, 2537–2553, https://doi.org/10.5194/essd-12-2537-2020, 2020a.

Landschützer, Peter; Laruelle, Goulven; Roobaert, Alizee; Regnier, Pierre: A combined global ocean pCO2 climatology combining open ocean and coastal areas (NCEI Accession 0209633). NOAA National Centers for Environmental Information. Dataset. doi: https://doi.org/10.25921/qb25-f418. Accessed [2020-04-08], 2020b.

Mason, E., Pascual, A., & McWilliams, J. C.: A New Sea Surface Height–Based Code for Oceanic Mesoscale Eddy Tracking. J. Atmos. Oceanic Technol., 31, 1181–1188, https://doi.org/10.1175/JTECH-D-14-00019.1, 2014.

McGillicuddy, D. J.: Mechanisms of Physical-Biological-Biogeochemical Interaction at the Oceanic Mesoscale. Annual Review of Marine Science (Vol. 8). https://doi.org/10.1146/annurev-marine-010814-015606, 2016.

McWilliams, J. C.: Submesoscale currents in the ocean. Proceedings of the Royal Society A: Mathematical, Physical and Engineering Sciences, 472(2189). https://doi.org/10.1098/rspa.2016.0117, 2016.

Mears, C.; Lee, T.; Ricciardulli, L.; Wang, X.; Wentz, F.: RSS Cross-Calibrated Multi-Platform (CCMP) 6-hourly ocean vector wind analysis on 0.25 deg grid, Version 3.0, Remote Sensing Systems, Santa Rosa, CA. Available at www.remss.com. https://doi.org/10.56236/RSS-uv6h30, 2022a.

Mears, C.; Lee, T.; Ricciardulli, L.; Wang, X.; Wentz, F.: Improving the Accuracy of the Cross-Calibrated Multi-Platform (CCMP) Ocean Vector Winds. *Remote Sens., 14*, 4230. https://doi.org/10.3390/rs14174230, 2022b.

Mongwe, N. P., Vichi, M., & Monteiro, P. M. S.: The seasonal cycle of p CO 2 and CO 2 fluxes in the Southern Ocean: diagnosing anomalies in CMIP5 Earth system models. Biogeosciences, 15(9), 2851–2872. https://doi.org/10.5194/bg-15-2851-2018, 2018.

Nevison, C. D., Manizza, M., Keeling, R. F., Stephens, B. B., Bent, J. D., Dunne, J., et al.: Evaluating CMIP5 ocean biogeochemistry and Southern Ocean carbon uptake using atmospheric potential oxygen: Present-day performance and future projection. Geophysical Research Letters, 43(5), 2077–2085. https://doi.org/10.1002/2015GL067584, 2016.

Omand, M. M., D'Asaro, E. A., Lee, C. M., Perry, M. J., Briggs, N., Cetinić, I., & Mahadevan, A.: Eddy-driven subduction exports particulate organic carbon from the spring bloom. Science, 348(6231), 222–225. https://doi.org/10.1126/science.1260062, 2015.

Orsi, A. H., Whitworth, T. I., & Nowlin, W. D. J.: On the meridional extent and fronts of the Antarctic Circumpolar Current. Deep Sea Research Part I. https://doi.org/10.1016/0967- 0637(95)00021-W, 1995.

Resplandy, L., Lévy, M., D'Ovidio, F., & Merlivat, L.: Impact of submesoscale variability in estimating the air-sea CO2 exchange: Results from a model study of the POMME experiment. Global Biogeochemical Cycles, 23(1), 1–19. https://doi.org/10.1029/2008GB003239, 2009.

Ricciardulli, L.; Foltz, G.R.; Manaster, A.; Meissner, T.: Assessment of Saildrone Extreme Wind Measurements in Hurricane Sam Using MW Satellite Sensors. *Remote Sens. 14*, 2726. https://doi.org/10.3390/rs14122726, 2022.

Sabine, C., Sutton, A., Mccabe, K., Lawrence-Slavas, N., Alin, S., Feely, R., et al.: Evaluation of a new carbon dioxide system for autonomous surface vehicles. Journal of Atmospheric and Oceanic Technology. https://doi.org/10.1175/JTECH-D-20-0010.1, 2020.

Sarmiento, J. L., K. S. Johnson, L. A. Arteaga, S. M. Bushinsky, H. M. Cullen, A. R. Gray, R. M. Hotinski, T. L. Maurer, M. R. Mazloff, S. C. Riser, J. L. Russell, O. M. Schofield, and L. D. Talley: The Southern Ocean carbon and climate observations and modeling (SOCCOM) project: A review. *Progress in Oceanography*, *219*, https://doi.org/10.1016/j.pocean.2023.103130, 2023.

Shadwick EH, Wynn-Edwards CA, Matear RJ, Jansen P, Schulz E and Sutton AJ: Observed amplification of the seasonal CO2 cycle at the Southern Ocean Time Series. *Front. Mar. Sci.* 10:1281854.doi: 10.3389/fmars.2023.1281854, 2023.

Sutton, A. J., Sabine, C. L., Maenner-Jones, S., Lawrence-Slavas, N., Meinig, C., Feely, R. A., et al.: A high-frequency atmospheric and seawater $p\mathrm{CO_2}$ data set from 14 open-ocean sites using a moored autonomous system. *Earth System Science Data*, **6**(2), 353–366. https://doi.org/10.5194/essd-6-353-2014, 2014.

Sutton, A. J., Battisti, R., Maenner Jones, S., Musielewicz, S., Bott, R., & Osborne, J.: Surface underway measurements of partial pressure of carbon dioxide (pCO2), sea surface temperature, sea surface salinity and other parameters from Autonomous Surface Vehicle ASV_Saildrone1020 (EXPOCODE 32DB20190119) in the South Atlantic Ocean, South Pacific Ocean, Indian Ocean and Southern Ocean from 2019-01-19 to 2019-08-03 (NCEI Accession 0221912): NOAA National Centers for Environmental Information. https://doi.org/10.25921/6zja-cg56, 2020.

Sutton, A. J., Williams, N. L., & Tilbrook, B.: Constraining Southern Ocean CO2 flux uncertainty using uncrewed surface vehicle observations. Geophysical Research Letters, 48, e2020GL091748, https://doi.org/10.1029/2020GL091748, 2021.

Talley, L. D., Rosso, I., Kamenkovich, I., Mazloff, M. R., Wang, J., Boss, E., et al.: Southern Ocean Biogeochemical Float Deployment Strategy, With Example From the Greenwich Meridian Line (GO-SHIP A12). Journal of Geophysical Research: Oceans, 124(1), 403–431. https://doi.org/10.1029/2018JC014059, 2019.

Toggweiler, J. R.: Shifting westerlies. Science, 323(5920), 1434–1435. https://doi.org/10.1126/science.1169823, 2009.

Open Access Earth System Science Data Discussions

Viglione, G. A., Thompson, A. F., Flexas, M. M., Sprintall, J., & Swart, S.: Abrupt transitions in submesoscale structure in Southern Drake Passage: Glider observations and model results. Journal of Physical Oceanography, 48(9), 2011–2027. https://doi.org/10.1175/JPO-D-17-0192.1, 2018.

Wanninkhof, R., Johnson, K., Williams, N., Sarmiento, J., Riser, S., Briggs, E., et al.: An evaluation of pH and NO3 sensor data from SOCCOM floats and their utilization to develop ocean inorganic carbon products: A summary of discussions and recommendations of the Carbon Working Group (CWG) of SOCCOM. Retrieved from http://soccom.princeton.edu/sites/default/files/files/CWG_white_paper_March_13_2016.pd f, 2016.

Wanninkhof, Rik: Relationship between wind speed and gas exchange over the ocean revisited. Limnology and Oceanography: Methods, 12(6), 351–362. https://doi.org/10.4319/lom.2014.12.351, 2014.

Whalen, C. B., MacKinnon, J. A., & Talley, L. D.: Large-scale impacts of the mesoscale environment on mixing from wind-driven internal waves. Nature Geoscience, 11(11), 842– 847. https://doi.org/10.1038/s41561-018-0213-6, 2018.

Williams, N L, Juranek, L. W., Johnson, K. S., Feely, R. A., Riser, S. C., Talley, L. D., et al.: Empirical algorithms to estimate water column pH in the Southern Ocean. Geophysical Research Letters, 43(7), 3415–3422. https://doi.org/10.1002/2016GL068539, 2016.

Williams, Nancy L., Juranek, L. W., Feely, R. A., Johnson, K. S., Sarmiento, J. L., Talley, L. D., et al.: Calculating surface ocean pCO2 from biogeochemical Argo floats equipped with pH: An uncertainty analysis. Global Biogeochemical Cycles, 31(3), 591–604. https://doi.org/10.1002/2016GB005541, 2017.

Williams, N. L., Juranek, L. W., Feely, R. A., Russell, J. L., Johnson, K. S., & Hales, B.: Assessment of the Carbonate Chemistry Seasonal Cycles in the Southern Ocean from Persistent Observational Platforms. Journal of Geophysical Research: Oceans, 123(7), 4833–4852. https://doi.org/10.1029/2017JC012917, 2018.

Zhang, D., Cronin, M. F., Meinig, C., Thomas Farrar, J., Jenkins, R., Peacock, D., et al.: Comparing air-sea flux measurements from a new unmanned surface vehicle and proven platforms during the spurs-2 field campaign. Oceanography, 32(2), 122–133. https://doi.org/10.5670/oceanog.2019.220, 2019.